Global Theory of Microtearing Modes in the Tokamak Pedestal

J. L. Larakers, M. Curie, D. R. Hatch, R. D. Hazeltine, and S. M. Mahajan

Phys. Rev. Lett. **126**, 225001 — Published 4 June 2021

DOI: 10.1103/PhysRevLett.126.225001

Global theory of micro-tearing modes in the tokamak pedestal

J.L. Larakers,* M. Curie, D.R. Hatch, R.D. Hazeltine, and S.M. Mahajan

Institute for Fusion Studies, University of Texas, Austin, TX 78712, USA

(Dated: April 20, 2021)

Abstract

The pedestal of H-mode tokamaks display strong magnetic fluctuations correlated with the evolution of the electron temperature. The micro-tearing mode (MTM)a temperature-gradient-driven instability that alters magnetic topologyis compatible with these observations. Here we extend the conventional theory of the MTM to include the global variation of the temperature and density profiles. The offset between the rational surface and the location of the pressure gradient maximum (μ) emerges as a crucial parameter for MTM stability. The extended theory matches observations on the JET tokamak.

INTRODUCTION

The high confinement (H-mode) operating regime of tokamaks offers a promising avenue for an effective fusion reactor. The essential characteristic of H-mode is the presence of a narrow region at the edge of the plasma where heat and particle transport is greatly diminished. This region is known as the pedestal. Due to its insulating properties, the pedestal is characterized by steep gradients in temperature and density.

A steep and stable pedestal is highly desirable. The pedestal's large gradients levitate the core plasma temperature and density profiles, improving the temperature and density for fusion reactions. Understanding the mechanisms that abate or even disrupt the pedestal is a prominent goal in the fusion community. The pedestal is also highly dynamic. Its evolution is quasi-periodic with a period of gradient steepening followed by a sudden crash of the gradients. These crashes are experimentally termed edge localized modes (ELMs).

During the gradient steepening cycle, the pedestal hosts a spectrum of saturated fluctuations. Figure 1 displays a typical magnetic spectrogram throughout the ELM cycle from the JET-C tokamak. During the inter-ELM period, the spectrogram displays discrete frequency bands of definite toroidal mode number (n). The frequency bands are a common feature of H-mode pedestals [1–6].

These bands have frequencies close to the diamagnetic frequency ($\omega_{*n} = k_\perp \rho_i v_i \ln(n)'/2$) and collision frequency ($\nu = \sqrt{2}\pi n e^4 \ln(\Lambda)/m_e^{1/2} T^{3/2}$): $\omega \sim \omega_{*n} \sim \nu$. Here T is the plasma temperature, n the density, $v_i = \sqrt{2T/m_i}$, $\rho_i = v_i/\Omega_i$ the ion gyro-radius, $k_\perp = m/r$, m the poloidal mode number, and $\ln(\Lambda)$ the Coulomb logarithm. r is the minor radial coordinate and the prime represents a radial derivative. The fluctuations occur in the presence of large temperature gradients, correlate with electron heat transport, and have long wavelengths $k_\perp \rho_i < 1$ [6]. All of these characteristics match the fingerprint of an instability known as the micro-tearing mode. [7]

The micro-tearing mode[8] (MTM) is an electromagnetic instability that is localized about rational magnetic surfaces and is capable of altering the flux-surface topology. Its growth rate scales with $\omega_{*T} = k_\perp \rho_i v_i \ln(T)'/2$. The real frequency is in the electron direction and is not far from the local diamagnetic frequency: $\omega \approx \omega_{*n} + \omega_{*T}$. It is distinctive from conventional tearing modes[9] by being driven by temperature gradients, with little regard for the conventional stability parameter Δ'[9], and in its dependence on the velocity variation of the Coulomb cross-section.[8]

The pedestal has many low-order rational surfaces discretely spaced on which micro-tearing modes could be active. Local gyrokinetic simulations and conventional MTM dispersion relations commonly predict all low-order rational surfaces as unstable[7, 10]. In contrast, global gyro-kinetic simulations show that only a subset of rational surfaces have active MTMs. [7, 10, 11] Micro-instabilities are known to be affected by global treatment [12–14]. Motivated by this circumstance, and a need for physical understanding, we extend the conventional MTM theory to include global effects.

The key global feature is the strong variation of the drift frequencies ω_{*n} and ω_{*T}, henceforth together referred to as ω_*, in the pedestal. The ω_* variation is non-monotonic. It is maximal near the mid pedestal, and away from the peak it decays. Despite the many theoretical studies of micro-tearing[8, 15–20] and more recent gyrokinetic simulations [12, 21–24], a basic analytical investigation of the impact of global ω_* variation on the MTM is not available.

The aforementioned gyrokinetic studies [10, 11] analyzed the unstable rational surfaces and found that they all lie near the peak in ω_*. This observation has demonstrated considerable power in explaining the distinctive fluctuation bands[6]. The rational surfaces that are radially offset from the peak are stable and lead to gaps in frequency and mode number. We term this observation 'offset stabilization'. In this Letter, we present an analytical and numerical study of the electromagnetic equations to explain offset stabilization. The results match with both gyrokinetic simulations and experimental data. This provides additional evidence that MTMs are the major source of magnetic fluctuations and transport in between ELMs.

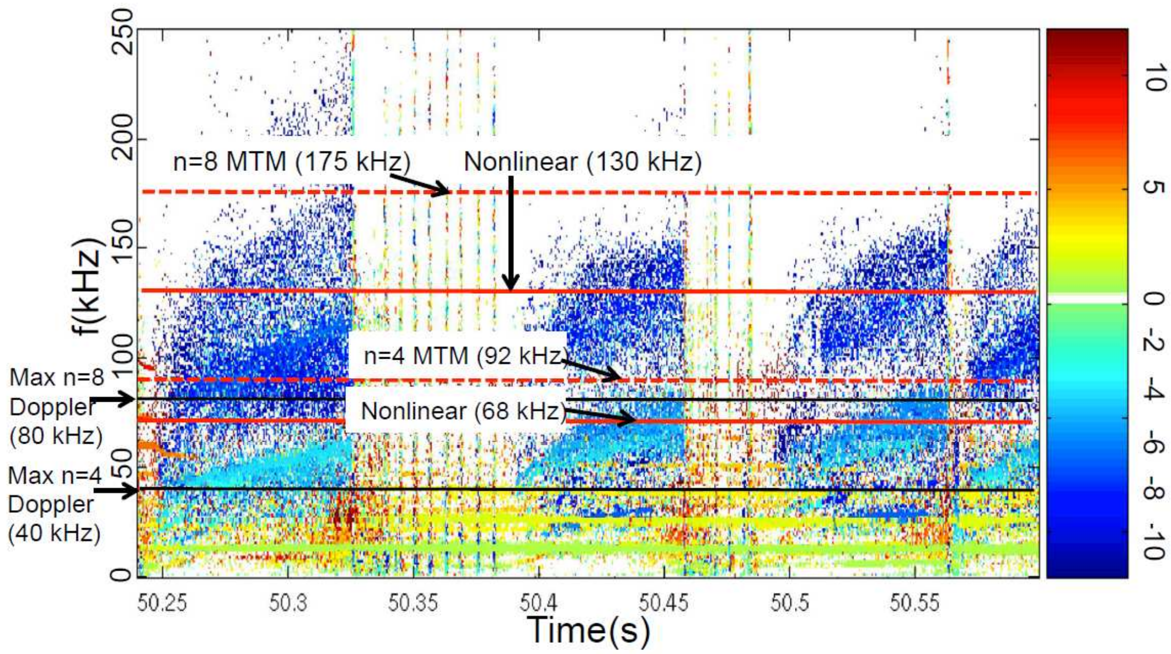

FIG. 1. Magnetic spectrogram showing fluctuations throughout several ELM cycles from JET-C pulse #78697. The vertical broadband lines are ELMs. The inter-ELM bands of fluctuations with toroidal mode numbers $n = -4$ and $n = -8$ are clearly visible. The negative sign indicates the mode is propagating in the electron diamagnetic direction. The low frequency bands with positive n numbers are core modes and not relevant to our study. Figure courtesy of Ref. [10].

There are two physical reasons for offset stabilization: (i) At the peak in ω_{*T} the driving energy is maximized. (ii) The ω_* profile and magnetic shear profile modulate the spatial structure of the mode. If the rational surface and the peak in ω_* align, these influences cooperate to trap the mode and enhance its growth rate. If the rational surface and the ω_* peak do not align, these influences compete and diminish the mode.

SET UP

Unconstrained motion along field lines allows magnetic surfaces to arrive at local thermal equilibrium on a fast time scale R/v_e. Here $v_e = \sqrt{2T/m_e}$ and R is the major radius. Slower transport across surfaces set ups radial gradients. Here by radial we mean the direction across magnetic surfaces. The micro-tearing mode is an instability about this quasi-stationary state.

We neglect the curvature of the toroidal geometry. This effectively brings our model into a Cartesian slab. We define x to be the radial direction and the origin $x = 0$ to coincide with a rational surface of interest. The perpendicular directions y and z lie in the planes of the magnetic surfaces. The z direction coincides with the direction of the magnetic field on the rational surface.

The magnetic field direction changes radially. We define $1/L_s = (r/qR)(\ln q)'$, $1/L_n = (\ln n)'$, and $1/L_T = (\ln T)'$ to characterize the magnetic shear and the quasi-stationary gradients; q is the safety factor. The dimensionless quantities $\hat{s} = L_n/L_s$, $\beta = 8\pi n_e T/B^2$, and $\eta = L_n/L_T$ will also be utilized.

The micro-tearing mode arises from the solution to suitably ordered versions of Ampere's law and quasi-neutrality ($\rho_i/a << 1, \omega \sim \omega_{*n} \sim \nu, \beta << 1, k_\perp \rho_i << 1$). a is the minor radius of the tokamak. These equations describe an electromagnetic perturbation with wave vector $\mathbf{k} = k_\perp \hat{y}$ and frequency ω. They have been repeatably discussed in the past literature. [8, 17, 18]

$$\frac{d^2 A_\parallel}{dx^2} = -\frac{4\pi}{c}\sigma_\parallel(\omega, x)E_\parallel \tag{1}$$

$$\left(\frac{c}{v_A}\right)^2 \omega(\omega - \omega_{*n})\frac{d^2\Phi}{dx^2} = -4\pi k_\parallel \sigma_\parallel(\omega, x)E_\parallel \tag{2}$$

Here $E_\parallel = i\omega A_\parallel/c - ik_\parallel\phi$ and $k_\parallel = \hat{b} \cdot \mathbf{k}$. Due to magnetic shear, $k_\parallel$ varies in the radial direction. It can be shown that $k_\parallel = k_\perp x/L_s$. The perturbed densities of quasi-neutrality (2) and the conductivity $\sigma_\parallel$ have been computed using kinetic theory. With boundary conditions on $A_\parallel$ and Φ, this becomes a generalized eigenvalue problem. The micro-tearing mode is a single branch of solutions. It has the largest growth rate in the parameter regime of interest.

For our analysis, we normalize all length scales to $\rho_s = \sqrt{2}\rho_i$ and frequencies to a representative value of ω_{*n}. The equations become.

$$\epsilon\frac{d^2\psi}{dx^2} = \sigma(\psi - x\phi) \tag{3}$$

$$\epsilon\frac{d^2\phi}{dx^2} = \frac{2x}{\omega(\omega - \omega_{*n})}\delta\sigma(\psi - x\phi) \tag{4}$$

Where $\psi = \omega A_\parallel$ and $\phi = \hat{s}c/v_i\Phi$. We can identify $\epsilon = m_e/(m_i\beta)$ and $\delta = \hat{s}^2/\beta$ as small parameters. Here ϵ is a conventional small parameter in fusion plasmas and δ is the inverse of a large parameter, $\hat{\beta}$, known to be important to the MTM[25].

The normalized conductivity σ is computed from the electron drift-kinetic equation[26]. It has the form.

$$\sigma(\omega, x) = i\Big((\omega - \omega_{*n}(x) - \omega_{*T}(x))L_{11} - \omega_{*T}(x)L_{12}\Big) \tag{5}$$

Here the "transport coefficients", L_{11} and L_{12} are functions of $k_\parallel v_e$, ν, and ω. The $k_\parallel$ dependence arises from the fact that particles respond differently to perturbations along the magnetic field and perpendicular to it. These functions contain the entire spectrum of electron response from adiabatic ($k_\parallel v_e >> \omega, \nu$) to resonant ($\omega \sim k_\parallel v_e$) to hydrodynamic ($\omega, \nu >> k_\parallel v_e$)[26]. Since $k_\parallel$ is spatially varying, all three of these regimes can be sampled by the MTM. These transport coefficients vary with a characteristic length scale $x_\sigma = \omega L_s/k_\perp v_e$; they are localized about the rational surface, decaying to zero at large $k_\parallel$. Clearly, magnetic shear controls the size of x_σ.

Clearly, the spatial variation of ω_* will effect σ. We denote the length scale of ω_* variation by x_*. This length scale is intimately tied to the width of the pedestal, and of the same order. The effect of the ω_* profile on the mode will increase as the ratio $r = x_\sigma/x_*$ increases. A survey of H-mode pedestals, discussed in the following section, has determined that this ratio ranges from 0.02 to 0.6 in the pedestal. Even for small values of this ratio, including the global spatial dependence is important in determining the stability. The spatial dependence of ω_* typically breaks the even/odd symmetry of the micro-tearing mode equations.

REDUCTION

Above we claimed that the ω_* profile and shear profile act together to determine the spatial structure of the mode. Here we exploit the small parameters ϵ and δ to support this claim. Our ordering restricts ourselves to modes which have length scales $w \gtrsim \rho_s$, where w is the radial mode width. To balance the smallness of ϵ, it follows that.

$$\sigma(\omega) \lesssim \epsilon \tag{6}$$

Formally, to zeroth order in ϵ the dispersion relation becomes $\sigma(\omega) = 0$, a well known result, and the original MTM dispersion relation [7, 8].

We proceed to higher order. Using $x \sim x_\sigma$ and $\sigma \sim \epsilon$ as upper limits, we see that the right hand side of (4) is $\mathcal{O}(\delta^{1/2}\epsilon^{3/2})$. To first order $\phi = 0$, and we are left with the equation.

$$\frac{d^2\psi}{dx^2} - \frac{1}{\epsilon}\sigma(x, \omega)\psi = 0 \tag{7}$$

This equation is conveniently in the form of a Schrödinger equation, in which σ/ϵ acts as a potential.

By plotting the structure of σ we find that alignment of the ω_* peak and the rational surface lead to cooperation and a deeper, stronger well. An offset weakens the well and dampens the mode.

NUMERICAL SOLUTION

We now proceed to the full numerical solution of (1) and (2). Our numerical solution is a 3-point stencil finite difference scheme. The discrete system is set up as a homogeneous linear problem with an unknown eigenvalue in the matrix. The eigenvalue ω appears in a nonlinear way in the equations (through σ). A secant method is applied to compute the eigenvalue. [27] We compute tearing parity eigenfunctions and enforce that the eigenfunctions are zero at a sufficient distance from the rational surface. When there is even/odd symmetry breaking, we identify MTMs by continuity with the symmetric case.

The conductivity model is taken from recent work [26]. It is in the form of a matrix-valued continued fraction, derived from projecting the drift-kinetic equation–including the full collision operator–into Sonine polynomials. Truncation at five Legendre polynomials and seven Laguerre polynomials gives good convergence. Our code has been bench-marked with previous work [16] by using the Lorentz Gas conductivity.

To study these equations a parameter survey was performed. It included ten H-mode pedestals from DIIID and JET-C. The parameters were computed using an equilibrium reconstruction of the temperature, density, and q profile with the code E-FIT. [28, 29] The reconstruction is time-averaged over the ELM cycle. The survey provided these parameter ranges: $\hat{s} : (0.005, 0.05), \eta : (1.0, 3.5), \beta : (0.0005, 0.002), \nu/\omega_* : (0, 10), x_*/\rho_s : (7.0, 20.0)$

ω_* VARIATION

The spatial variation of ω_* in the pedestal is modeled by

$$\omega_{*n}(x) + \omega_{*T}(x) = \omega_{\text{peak}} \exp\left(\frac{-(x-\mu)^2}{x_*^2}\right) \tag{8}$$

Since $x = 0$ is the position of the rational surface, μ represents a displacement of the peak in ω_* from that surface. For simplicity, we assume ω_{*n} and ω_{*T} have the same spatial

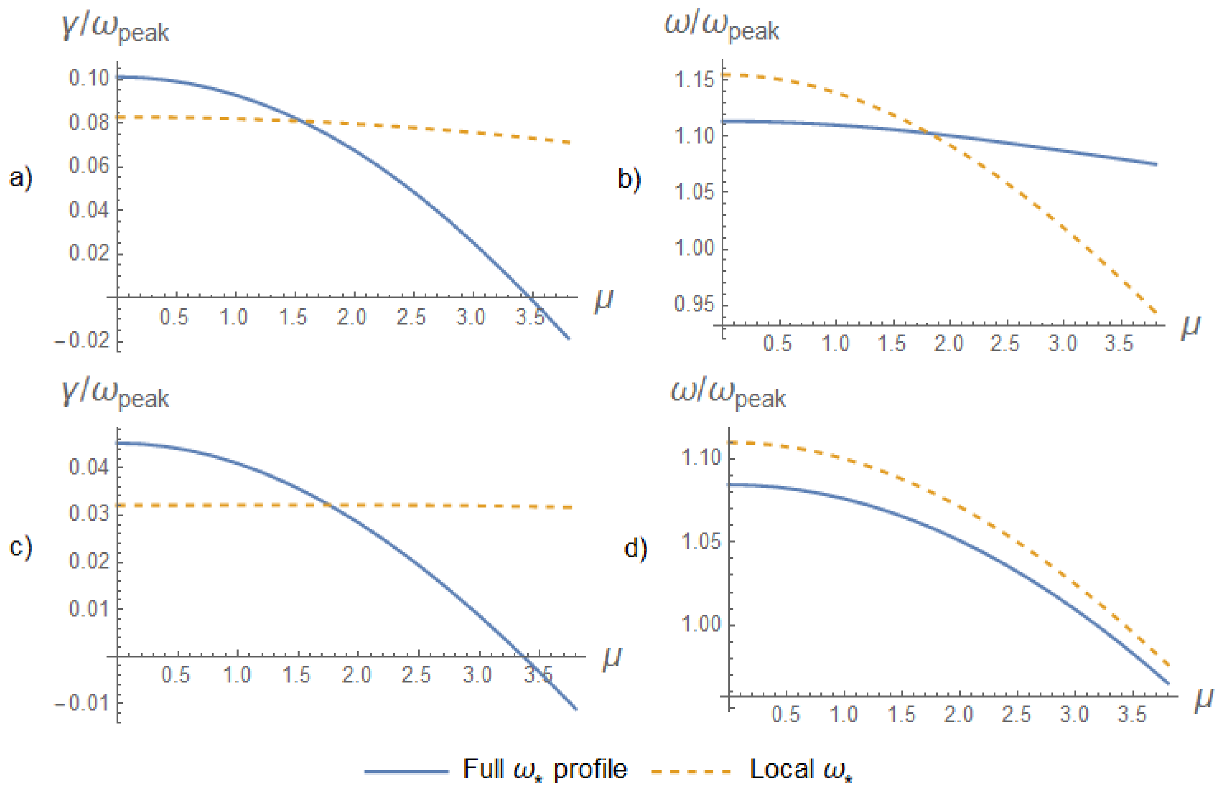

FIG. 2. Growth rate and real frequency of the mode as μ is increased. The blue line indicates the growth rate computed using the full spatial dependence of ω_*. The orange line (dotted) shows the growth rate if ω_* is evaluated at the rational surface and treated as uniform (i.e., the local approximation). (a) & (b) show the eigenvalue corresponding to $r = 0.28$ and $\hat{s} = 0.006$, (c) & (d) correspond to $r = 0.14$ and $\hat{s} = 0.012$. Other parameters are set to: $x_*/\rho_s = 10.0, \beta = 0.002, \nu/\omega_{peak} = 1.0, \eta = 2.0$.

dependence, a circumstance that is appropriate in the pedestal.

We solve (3) and (4) numerically and vary μ and r. To elucidate the necessity of ω_* variation, we compute the growth rate with the full dependence given in (8) and contrast it to uniform ω_*. The uniform ω_* value is determined by evaluating (8) at the local position of the rational surface.

Figure 2 contrasts the scans for different r values and the different ω_* treatments. It is clear that the local uniform approximation does not match the more accurate full spatial variation. We observe offset stabilization: the MTM is only unstable when the rational surface is near the peak in ω_*.

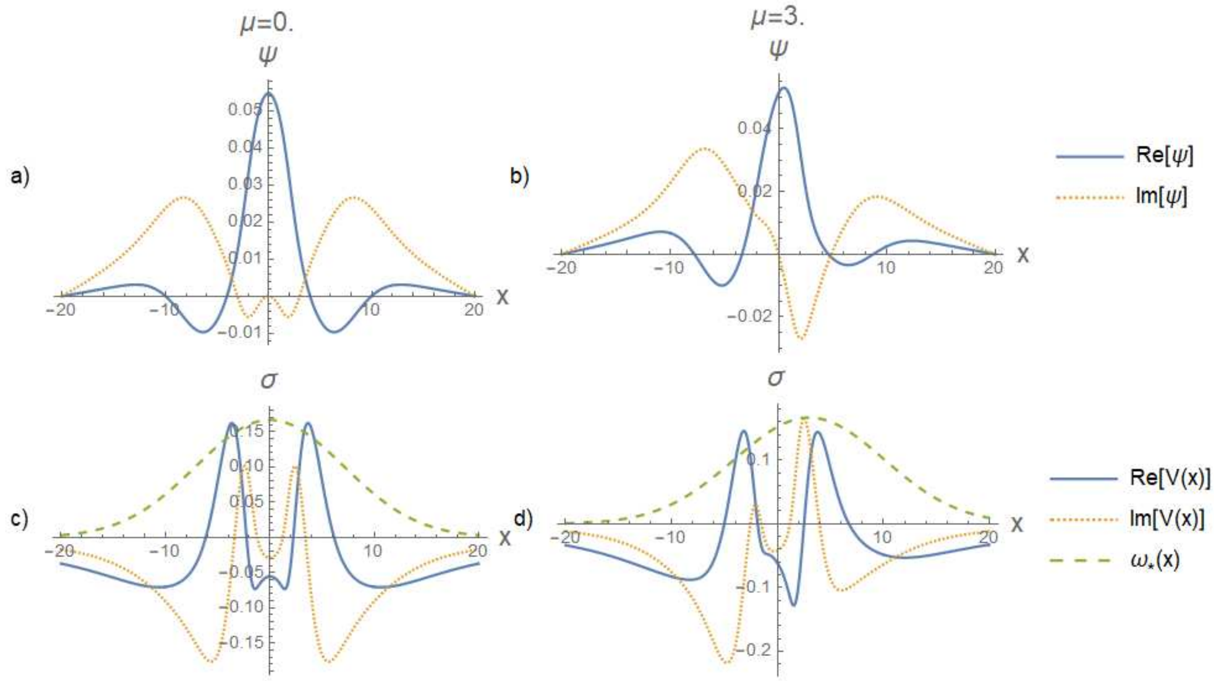

FIG. 3. The eigenmode and the conductivity evaluated at ω (a) & (c) correspond to the rational surface and ω_* peak aligning and (b) & (d) correspond to an offset of $\mu = 3.0$. The eigenvalues were determined to be $\omega/\omega_{peak} = 1.084 + 0.045i$ and $\omega/\omega_{peak} = 1.009 + 0.009i$ respectively. Parameters were set to: $x_*/\rho_s = 10.0, \beta = 0.002, \hat{s} = 0.012, \nu/\omega_{peak} = 1.0, \eta = 2.0, Z_{eff} = 1.0, m_i/m_e = 1836$. Here $V(x) = i\sigma$.

Figure 3 displays the eigenfunctions and the conductivity when the peak in ω_* aligns and when it does not. The plots show how ω_* profile influences σ and how the conductivity influences the eigenmode.

COMPARISON WITH JET OBSERVATIONS

We conclude by comparing our model to a recently published gyro-kinetic study and experimental spectrogram of JET-C shot #78697 (shown in Figure 1)[10]. The gyrokinetic simulations were performed using the code GENE[30, 31] including the entire toroidal magnetic geometry. Realistic radial profiles of electron temperature, q, inter alia, were computed from experimental diagnostics. The study performed both global linear simulations–considering poloidal mode coupling and profile variation–and local linear simulations. To establish matching of the simulations with the experimental spectrogram, the nominal equi-

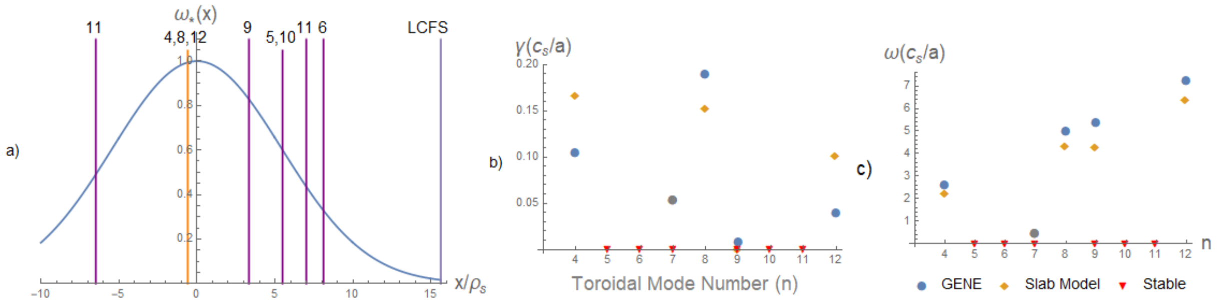

FIG. 4. Here we display the comparison of the slab model to global linear GENE. (a) Displays the Gaussian fit of the ω_* profile and the location of the rational surfaces determined from the q profile. (b) Displays the growth rates of each toroidal mode number. (c) Displays the real frequencies of the unstable modes. The stable markers indicate a negative growth rate for both the slab model and GENE (excluding $n = 7$ and $n = 9$). $n = 7$ (grey) is predicted to be unstable by GENE, however due to the large jump in real frequency, inter-alia, it is not a MTM. $n = 9$ is predicted to be unstable by GENE, but the growth rate is marginal.

librium profiles were modified within the error bars. The temperature gradient was increased by 20% and the q profile was reduced by 5%. The local linear simulations computed unstable MTMs at all low-order rational surfaces while the global simulations selected only the rational surface near the peak in ω_* as unstable.

To perform a comparison of these results to our model, we fit the ω_* profile to a Gaussian and located the positions of rational surfaces with the q profile. Local values of $\hat{s}$, β, ν and η were extracted for each rational surface; the full variation of these parameters was shown to insignificantly effect the growth rates. Growth rates were computed for each rational surface using both uniform and non-uniform ω_*. Under the uniform approximation, all of the toroidal mode numbers (up to 12) were found to be unstable.

Global linear GENE [10] and our global reduced model both indicate that only the rational surface $q = 2.75$ associated with $n = 4, 8, 12$ is unstable. Figure 4 provides a full comparison. The $n = 4$ and $n = 8$ modes are observed in the magnetic spectrogram. The real frequencies from linear simulations slightly overestimate the frequency of the fluctuations. Nonlinear simulations performed in [10] provides corrections to capture the proper frequency. The $n =$ 12 mode does not appear in the magnetic spectrogram (likely due to the more rapid decay of magnetic fluctuations at smaller scales[10]). Beyond these considerations, the observation that solely $n = 4$ and $n = 8$ fluctuations appear provides evidence that these discrete fluctuation bands arise from micro-tearing modes.

Because of the large experimental uncertainty in the q profile (up to 20% relative error[32]), the locations of the rational surfaces are not known to great precision (approximately $10\rho_s$). Consequently, the framework described here should not be interpreted as having the capability of predicting frequency bands but rather the ability to reproduce them within experimental uncertainties.

CONCLUSION

In this Letter, we have extended the conventional theory of micro-tearing modes by including the global variation of the ω_* profiles. We have demonstrated that the ω_* profile and the magnetic q profile form the potential well of the mode. The q profile enters by virtue of the spatial dependence of the non-adiabatic electron response $L_{1i}(k_\parallel(x))$.

This extension has proven to be fruitful. Our model identifies a crucial and until now unknown parameter for the stability of the MTM. It was shown that displacement (μ) of the rational surface from the peak in ω_* quickly stabilizes the mode. We reason this is due to the breakdown of the potential well. This leads to a simple yet powerful condition for MTM instability in the pedestal: the rational surface must lie near the peak in ω_* for it to be unstable.

Armed with this extended model, we produced additional evidence that micro-tearing modes are a major source of magnetic fluctuations during the inter-ELM cycle. We examined and compared our model to a spectrogram from JET. Our model predicts the same frequency bands and mode numbers as unstable. The unstable mode numbers correspond to rational surfaces which nearly align with the ω_* peak. The uniform ω_* approximation, in contrast, predicts all mode numbers as unstable and a broadband spectrum of magnetic fluctuations. The vast differences in the global and local predictions nullifies local treatments for studying MTM stability in the pedestal.

These results provide a simple and expedient framework for determining if micro-tearing modes are the source of magnetic fluctuations in the pedestal. Future work will focus on applying this framework to larger data sets to solidify this hypothesis. A solid understanding of these fluctuations is a necessary ingredient for modelling the structure and evolution of the pedestal.

We thank Ehab Hassan for his encouragement and for his assistance gathering pedestal parameters. This work was supported by the Department of Physics, University of Texas at Austin and by the U.S. Department of Energy, Grant Numbers DOE ER54742, ER54698, and CH11466.

---

* j_larakers@utexas.edu.

[1] C. P. Perez, H. R. Koslowski, T. C. Hender, P. Smeulders, A. Loarte, P. J. Lomas, G. Saibene, R. Sartori, M. Becoulet, T. Eich, R. J. Hastie, G. T. Huysmans, S. Jachmich, A. Register, and F. C. Schüller, Washboard modes as ELM-related events in JET, Plasma Physics and Controlled Fusion **46**, 61 (2004).

[2] A. Diallo, J. W. Hughes, M. Greenwald, B. Labombard, E. Davis, S. G. Baek, C. Theiler, P. Snyder, J. Canik, J. Walk, T. Golfinopoulos, J. Terry, M. Churchill, A. Hubbard, M. Porkolab, L. Delgado-Aparicio, M. L. Reinke,A. White, and AlcatorC-Modteam, Observation of edge instability limiting the pedestal growth in Tokamak plasmas, Physical Review Letters **112**, 115001 (2014).

[3] A. Diallo, R. J. Groebner, T. L. Rhodes, D. J. Battaglia, D. R. Smith, T. H. Osborne, J. M. Canik, W. Guttenfelder, and P. B. Snyder, Correlations between quasi-coherent fluctuations and the pedestal evolution during the inter-edge localized modes phase on DIII-D, Physics of Plasmas **22**, 10.1063/1.4921148 (2015).

[4] M. Cavedon, R. Dux, T. Pütterich, E. Viezzer, E. Wolfrum, M. Dunne, E. Fable, R. Fischer, G. F. Harrer, F. M. Laggner, A. F. Mink, U. Plank, U. Stroth, M. Willensdorfer, and A. Upgrade Team, On the ion and electron temperature recovery after the ELM-crash at ASDEX upgrade, Nuclear Materials and Energy **18**, 275 (2019).

[5] F. M. Laggner, A. Diallo, M. Cavedon, and E. Kolemen, Inter-ELM pedestal localized fluctuations in tokamaks: Summary of multi-machine observations, Nuclear Materials and Energy **19**, 479 (2019).

[6] A. Diallo and F. M. Laggner, Review: Turbulence dynamics during the pedestal evolution between edge localized modes in magnetic fusion devices, Plasma Physics and Controlled Fusion 10.1088/1361-6587/abbf85 (2020).

[7] M. Kotschenreuther, X. Liu, D. R. Hatch, S. Mahajan, L. Zheng, A. Diallo, R. Groebner, J. C. Hillesheim, C. F. Maggi, C. Giroud, F. Koechl, V. Parail, S. Saarelma, E. Solano, and A. Chankin, Gyrokinetic analysis and simulation of pedestals to identify the culprits for energy losses using 'fingerprints', Nuclear Fusion **59**, 10.1088/1741-4326/ab1fa2 (2019), arXiv:1903.09994.

[8] R. D. Hazeltine, D. Dobrott, and T. S. Wang, Kinetic theory of tearing instability, Physics of Fluids **18**, 1778 (1975).

[9] H. P. Furth, J. Killeen, and M. N. Rosenbluth, Finite-resistivity instabilities of a sheet pinch, Physics of Fluids **6**, 459 (1963).

[10] D. R. Hatch, M. Kotschenreuther, S. M. Mahajan, M. J. Pueschel, C. Michoski, G. Merlo, E. Hassan, A. R. Field, L. Frassinetti, C. Giroud, J. Hillesheim, C. F. Maggi, C. P. von Thun, C. M. Roach, S. Saarelma, D. Jarema, and F. Jenko, Microtearing modes as the source of magnetic fluctuations in the jet pedestal, Nuclear Fusion (2020).

[11] E. Hassan, D. Hatch, G. Merlo, M. Halfmoon, M. Curie, M. Kotschenreuther, S. Mahajan, R. Groebner, and A. Diallo, Microtearing Signatures in DIII-D Pedestal, preprint **N/A**, N/A (2020).

[12] D. Dickinson, *Effects of profiles on microinstabilities in tokamaks*, Ph.D. thesis, University of York (2012).

[13] G. L. Falchetto, J. Vaclavik, and L. Villard, Global-gyrokinetic study of finite β effects on linear microinstabilities, Physics of Plasmas **10**, 1424 (2003).

[14] P. A. Abdoul, D. Dickinson, C. M. Roach, and H. R. Wilson, Using a local gyrokinetic code to study global ion temperature gradient modes in tokamaks, Plasma Physics and Controlled Fusion **57**, 10.1088/0741-3335/57/6/065004 (2015).

[15] R. R. Dominguez, M. Rosenberg, and C. S. Chang, Nonlinear theory of high-m tearing modes, Physics of Fluids **24**, 472 (1981).

[16] N. T. Gladd, J. F. Drake, C. L. Chang, and C. S. Liu, Electron temperature gradient driven microtearing mode, Physics of Fluids **23**, 1182 (1980).

[17] J. F. Drake and Y. C. Lee, Kinetic theory of tearing instabilities, Physics of Fluids **20**, 1341 (1977).

[18] S. M. Mahajan, R. D. Hazeltine, H. R. Strauss, and D. W. Ross, Unified theory of tearing modes, Physics of Fluids **22**, 2147 (1979).

[19] R. D. Hazeltine and D. W. Ross, Variational theory of drift and tearing eigenmodes in slab geometry, Physics of Fluids **21**, 1140 (1978).

[20] A. Zocco, N. F. Loureiro, D. Dickinson, R. Numata, and C. M. Roach, Kinetic microtearing modes and reconnecting modes in strongly magnetised slab plasmas, Plasma Physics and Controlled Fusion **57**, 10.1088/0741-3335/57/6/065008 (2015).

[21] D. R. Hatch, M. Kotschenreuther, S. Mahajan, P. Valanju, F. Jenko, D. Told, T. Görler, and S. Saarelma, Microtearing turbulence limiting the JET-ILW pedestal, Nuclear Fusion **56**, 10.1088/0029-5515/56/10/104003 (2016).

[22] X. Jian, C. Holland, J. Candy, E. Belli, V. Chan, A. M. Garofalo, and S. Ding, Role of Microtearing Turbulence in DIII-D High Bootstrap Current Fraction Plasmas, Physical review letters **123**, 225002 (2019).

[23] W. Guttenfelder, J. Candy, S. M. Kaye, W. M. Nevins, E. Wang, R. E. Bell, G. W. Hammett, B. P. LeBlanc, D. R. Mikkelsen, and H. Yuh, Electromagnetic transport from microtearing mode turbulence, Physical Review Letters **106**, 155004 (2011).

[24] H. Doerk, F. Jenko, M. J. Pueschel, and D. R. Hatch, Gyrokinetic microtearing turbulence, Physical Review Letters **106**, 155003 (2011).

[25] J. F. Drake, T. M. Antonsen, A. B. Hassam, and N. T. Gladd, Stabilization of the tearing mode in high-temperature plasma, Physics of Fluids **26**, 2509 (1983).

[26] J. L. Larakers, R. D. Hazeltine, and S. M. Mahajan, A comprehensive conductivity model for drift and micro-tearing modes, Physics of Plasmas **27**, 1 (2020).

[27] M. H. Meylan and L. Gross, A parallel algorithm to find the zeros of a complex analytic function., ANZIAM Journal **44**, 236 (2008).

[28] O. Meneghini and L. Lao, Integrated modeling of tokamak experiments with OMFIT, Plasma and Fusion Research **8**, 1 (2013).

[29] O. Meneghini, S. P. Smith, L. L. Lao, O. Izacard, Q. Ren, J. M. Park, J. Candy, Z. Wang, C. J. Luna, V. A. Izzo, B. A. Grierson, P. B. Snyder, C. Holland, J. Penna, G. Lu, P. Raum, A. McCubbin, D. M. Orlov, E. A. Belli, N. M. Ferraro, R. Prater, T. H. Osborne, A. D. Turnbull, and G. M. Staebler, Integrated modeling applications for tokamak experiments with OMFIT, Nuclear Fusion **55**, 10.1088/0029-5515/55/8/083008 (2015).

[30] F. Jenko, W. Dorland, M. Kotschenreuther, and B. N. Rogers, Electron temperature gradient driven turbulence, Physics of Plasmas **7**, 1904 (2000).

[31] T. Görler, X. Lapillonne, S. Brunner, T. Dannert, F. Jenko, F. Merz, and D. Told, The global version of the gyrokinetic turbulence code GENE, Journal of Computational Physics **230**, 7053 (2011).

[32] W. Rowan and K. Gentle, private communications.